

Pharmaceutical and Pharmacological Evaluation of Amoxicillin after Solubility Enhancement Using the Spray Drying Technique

Faiza Hassan, Muhammad Sher,* Muhammad Ajaz Hussain, Mubshara Saadia, Muhammad Naeem-Ul-Hassan, Muhammad Fayyaz ur Rehman,* Muhammad Tahir Haseeb, Syed Nasir Abbas Bukhari, Azhar Abbas, Bo Peng, Fariha Kanwal, and Huibiao Deng*

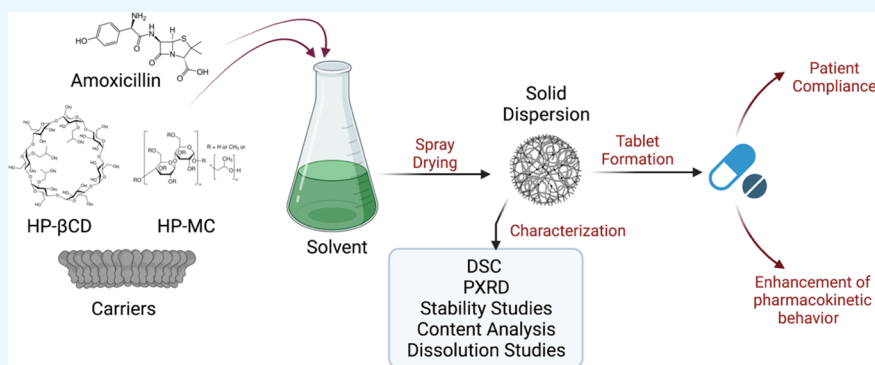
Cite This: *ACS Omega* 2022, 7, 48506–48519

Read Online

ACCESS |

Metrics & More

Article Recommendations



ABSTRACT: The dose frequency of drugs belonging to class II is usually high and associated with harmful effects on the body. The study aimed to enhance the solubility of the poorly water-soluble drug amoxicillin (AM) by the solid dispersion (SD) technique. Six different SDs of AM, F1–F6, were prepared by the spray drying technique using two other carriers, HP- β -CD (F1–F3) and HPMC (F4–F6), in 1:1, 1:2, and 1:3 drug-to-polymer ratios. These SDs were analyzed to determine their practical yield, drug content, and aqueous solubility using analytical techniques such as Fourier transform infrared spectroscopy, scanning electron microscopy, thermogravimetric analysis, and powder X-ray diffraction. The effect of polymer concentration on SDs was determined using aqueous solubility, *in vitro* dissolution, and *in vivo* studies. The results showed no drug–polymer interactions in SDs. Solubility studies showed that SDs based on the drug-to-polymer ratio of 1:2 (F2 and F5) were highly soluble in water compared to those with ratios of 1:1 and 1:3. *In vitro* dissolution studies also showed that SDs with a ratio of 1:2 released the highest drug concentration from both polymeric systems. The SDs based on HPMC confirmed the more sustained release of the drug as compared to that of HP- β -CD. All the SDs were observed as stable and amorphous, with a smooth spherical surface. *In vivo* studies reveal the enhancement of pharmacokinetics parameters as compared to standard AM. Hence, it is confirmed that spray drying is an excellent technique to enhance the solubility of AM in an aqueous medium. This may contribute to the enhancement of the pharmacokinetic behaviors of SDs.

1. INTRODUCTION

Amoxicillin (AM) is a semisynthetic penicillin derived from ampicillin and introduced at 1972.¹ AM is an effective remedy against Gram-positive and Gram-negative bacteria.² The toxicity level of the drug is very low,³ and it shows antibacterial activity by inhibiting the DD-transpeptidase, which maintains the integrity of the bacterial cell wall; consequently, the bacterial cell wall becomes fragile, leading to cell death.⁴ AM, combined with potassium salt of clavulanic acid, is marketed under the brand name “Augmentin”.⁵ Numerous side effects are associated with the treatment of AM, such as hypersensitivity, skin allergies, convulsions, erythematous rashes, Jarisch–Herxheimer reaction, and higher production of liver

enzymes.^{6–12} AM is slightly soluble in water and provides reduced bioavailability.¹³ Aqueous solubility is an important parameter to get the desired drug concentration in systemic circulation for the pharmacological response. A low aqueous solubility leads to a slow dissolution process that limits a drug’s absorption from the gastrointestinal tract.^{14–16} Therefore, to

Received: October 25, 2022
Accepted: November 28, 2022
Published: December 15, 2022



enhance the bioavailability of a drug, its solubility in water should be enhanced.^{16,17}

Cyclodextrins (CDs) are a family of three major cyclic oligosaccharides, α -CD, β -CD, and γ -CD, composed of six, seven, and eight glucopyranose units, respectively.¹⁸ CD consists of a hydrophilic outer surface with many hydrogen donors and acceptors and a central lipophilic cavity. Therefore, CDs do not infuse lipophilic membranes, while their inner cavity can host various hydrophobic agents.¹⁹ Hydroxypropylmethylcellulose (HPMC) is an *ortho*-(2-hydroxyl propylated) cellulose.²⁰ It is a nontoxic pharmaceutical excipient that acts as an emulsifier, film coating, thickening, and sustained-release agent in a number of tablets. It maintains the shelf life of the final product and reduces friability.^{21,22} Therefore, a constant drug release rate is achieved.²³ Consequently, patient compliance is achieved.

Recently, HP- β -CD and HPMC have been extensively used in the preparation of various formulations such as controlled-release pellets, microcapsules, matrix sustained-release tablets, and controlled-release tablets as complexing agents to enhance aqueous solubility and bioavailability of poorly water-soluble drugs.²⁴ This study proceeds to enhance the solubility and then bioavailability of AM. The effect of varying concentrations of the polymer has been determined with respect to *in vitro* drug release profiles and various other parameters. The study aims to achieve a higher drug concentration in plasma with more stable and extended therapeutic effects.

2. RESULTS AND DISCUSSION

2.1. Solid Dispersions. “Solid dispersions” (SDs) are a vital approach to achieve a drug dispersed amorphously in a polymeric matrix.³⁴ Six different SDs (F1–F6) based on AM and polymers HP- β -CD and HPMC were prepared by spray drying. SDs (F1–F6) appeared as a yellowish off-white amorphous powder with sticky nature.

2.2. Preliminary Studies of SDs. The practical yield ranged from 56 to 76% (Table 1). Formulation F5 was found

Table 1. Preliminary Studies of SDs F1–F6

sr. no.	SD code	practical yield (%)	DCs (%)	water solubility (mg mL ⁻¹)
1	F1	65.0 ± 1.05	87.8 ± 0.32	85.22
2	F2	75.0 ± 1.24	90.0 ± 0.65	88.06
3	F3	65.2 ± 1.11	84.8 ± 0.45	56.81
4	F4	56.6 ± 1.85	86.6 ± 0.27	79.11
5	F5	76.0 ± 1.45	89.7 ± 0.16	81.25
6	F6	70.0 ± 1.33	81.5 ± 0.54	65.70

to have the highest percent practical yield, that is, 76%, and formulation F4 was found to have the lowest percent practical yield, that is, 56.6%, compared with other formulations. The practical yield of SDs with a drug-to-polymer ratio of 1:2 was found to be the highest compared to those consisting of ratios 1:1 and 1:3. The percent yield (PY) of spray-dried SDs depends upon the drug-to-polymer ratio and the parameters of the spray drier, such as the inlet temperature, drying gas humidity, viscosity, and concentration of the feed solution.²⁵ As a result of higher inlet temperature, lower humidity of drying gas, lower viscosity of the feed solution, and higher evaporation rate of solvent, the formation of fine powder was achieved.

The drug content (DC) of the spray-dried SD varied between 81.50 and 90.0% (Table 1). The highest DC of 90.0% was observed with batch F2. A slight decrease in DC was observed upon increasing the concentration of the polymer in the SD. Our observations agreed with those of Kothari et al. (2015).²⁶ It was also noted that the use of high-molecular-weight polymers led to a higher feed viscosity. Similar observations were made by Auch et al. (2019) where the viscosity of the system was enhanced by increasing the concentration of the polymer.²⁷ As a result, the molecular movement of the drug hinders and leads to a lower loading of the drug in the polymer.

2.3. Aqueous Solubility Studies. The aqueous solubility of standard AM and SDs F1–F6 are presented in Figure 1. The

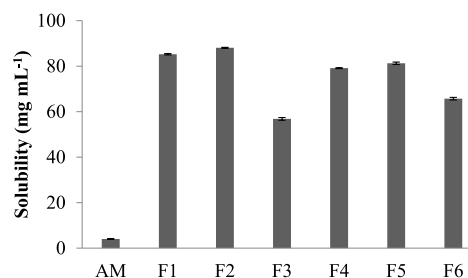


Figure 1. Solubility profile of AM and SDs F1–F6.

solubility data showed that the polymers, HP- β -CD and HPMC, enhanced the solubility of all the SDs compared to that of standard AM. Improved solubility levels were achieved due to the amorphous nature of the products, reduced particle size, and better wettability. Due to the amphiphilic nature of polymers, solubility levels of the SDs were enhanced by increasing the polymer ratio in SDs to 1:2. A drug in an amorphous state possesses a higher internal energy state than its crystalline state. As a result, the drug requires low energy to dissolve in an aqueous solution.^{28,29} Upon comparing polymers, it was found that the aqueous solubility was slightly enhanced by using HP- β -CD compared to HPMC.

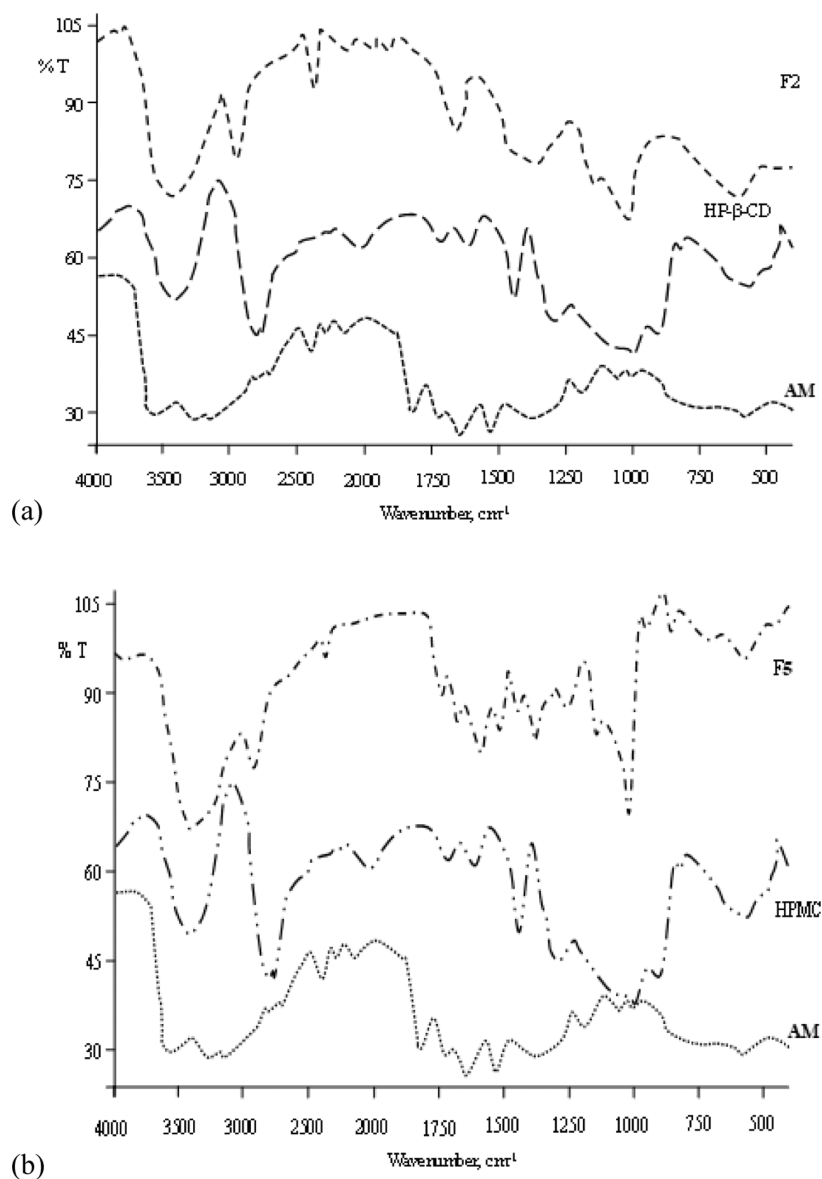
It was noted that the solubility of the SDs was decreased on increasing the drug–polymer concentration up to 1:3. The results were in agreement with those of Rajput et al. (2021), who attributed this behavior to the entrapment and then the suppression of drug molecules inside the polymer. When the polymer concentration increases, the viscosity of the gel also increases. Consequently, the diffusional path length is also lengthened. This leads to a reduction in the solubility rate.³⁰

2.4. Precompression Properties. The SDs of AM consisting of HP- β -CD showed better flow properties than those of HPMC. The values of loose bulk density and tapped bulk density for all the SDs of AM were in the range of 0.24 ± 0.12–0.45 ± 0.88 and 0.29 ± 0.06–0.62 ± 0.97 g mL⁻¹, respectively. The values of the angle of repose (AOR) were in the range of 25.74 ± 0.23 to 48.00 ± 0.76. The values of Hausner’s ratio ranged from 1.13 ± 0.05 to 1.37 ± 0.22, representing the good flow ability of SD powder. Carr’s index values ranged from 12.16 ± 0.03 to 27.27 ± 0.93 (%) for all the SDs of AM.

The determined values of precompression parameters of all the SDs indicated the flow properties within the acceptable limits, as shown in Table 2. The SDs of AM consisting of HP- β -CD displayed better flow properties than that of HPMC. F1 and F4 displayed the best flow characteristics. F2 and F5

Table 2. Rheological Properties of Drugs and SDs F1–F6

SDs	AOR (θ)	loose bulk density (g mL ⁻¹)	tapped bulk density (g mL ⁻¹)	Hausner ratio (%)	Carr's index
AM	40.49 ± 0.43	0.30 ± 0.05	0.38 ± 0.74	1.26 ± 0.16	21.21 ± 0.64
F1	25.74 ± 0.23	0.29 ± 0.65	0.33 ± 0.36	1.13 ± 0.05	12.16 ± 0.03
F2	33.26 ± 0.33	0.24 ± 0.12	0.29 ± 0.06	1.19 ± 0.84	16.39 ± 0.32
F3	44.00 ± 0.55	0.45 ± 0.88	0.62 ± 0.97	1.30 ± 0.04	27.27 ± 0.06
F4	30.20 ± 0.12	0.44 ± 0.32	0.48 ± 0.88	1.18 ± 0.04	8.42 ± 0.05
F5	35.00 ± 0.54	0.25 ± 0.08	0.30 ± 0.55	1.23 ± 0.03	18.75 ± 0.61
F6	48.00 ± 0.76	0.38 ± 0.98	0.52 ± 0.45	1.37 ± 0.22	27.27 ± 0.93

Figure 2. (a) FTIR spectra of HP- β -CD, AM, and F2. (b) FTIR spectra of HPMC, AM, and F5.

showed fair flow properties, whereas F3 and F6 showed poor flow properties. As the ratio of the polymer was increased, the flowability behavior was reduced due to the coating of the drug by the carrier. The small size of particles could tend to reduce the flow by increasing surface area per unit mass.³¹

2.5. Characterization. **2.5.1. FTIR Spectroscopy.** To evaluate any possible molecular interactions between the drug and polymer in each SD, AM, polymers HP- β -CD and HPMC, and the SDs were analyzed by FTIR spectroscopic

analysis using the KBr pellet method. The FTIR spectroscopy of polymers, drugs, and both SDs are presented in Figure 2a,b. The FTIR spectrum of HP- β -CD showed the vibration bands of CO and OH groups at 1136 and 1031 cm⁻¹, respectively, while the absorption bands of the OH group were at 3404 cm⁻¹. The FTIR spectrum of HPMC showed stretching vibrations of CH at 2887.44 cm⁻¹, OH group at 3464.15 cm⁻¹, CH₃ at 1456.26 cm⁻¹, and CO at 1041.56 cm⁻¹. The band at 1641.42 cm⁻¹ was due to the bending vibrations of H–OH

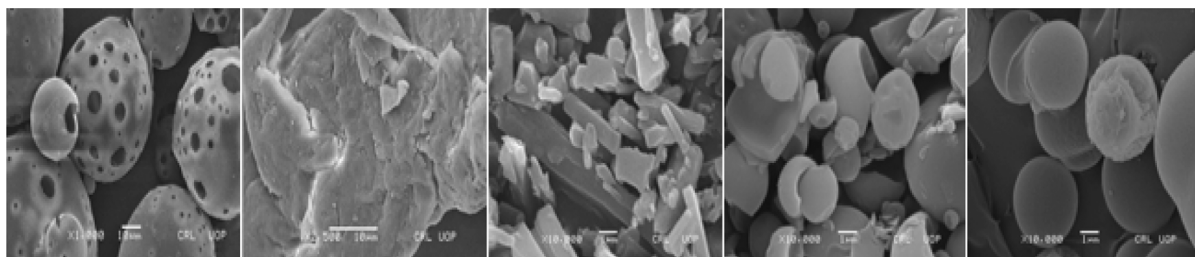


Figure 3. SEM images of samples; left to right: HP- β -CD, HPMC, AM, F2, and F5.

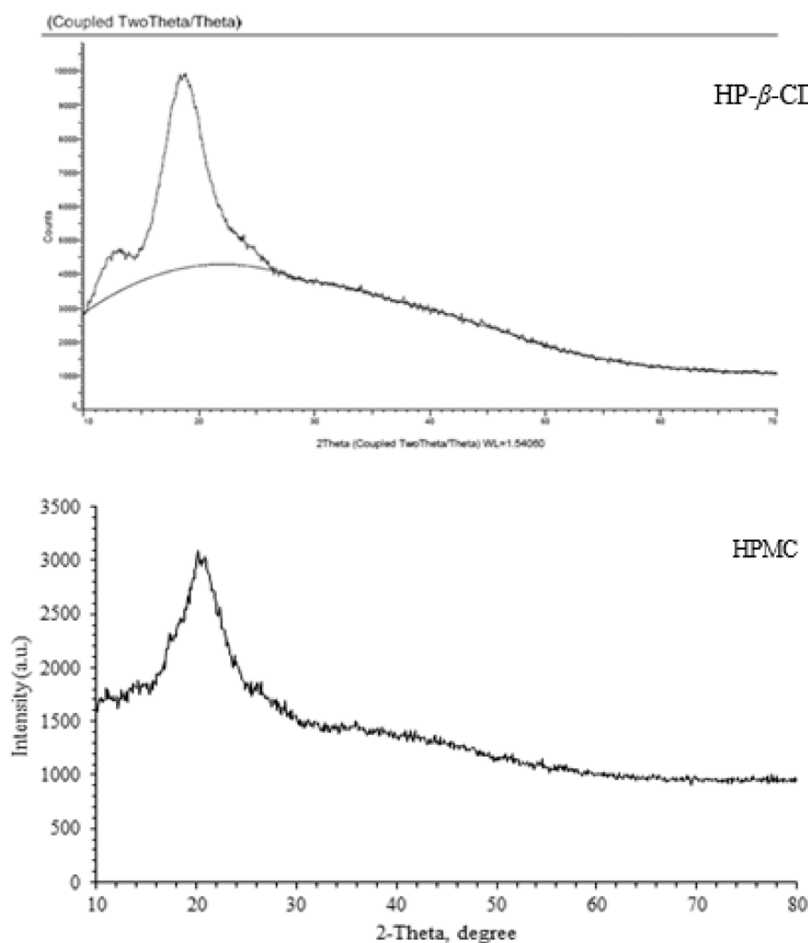


Figure 4. PXRD patterns of polymers, HP- β -CD and HPMC.

groups present in HPMC. The FTIR data obtained was found to be in good agreement with the work of peers.³²

The FTIR spectrum of AM showed strong absorption at 1766 cm^{-1} , characteristic of the β -lactam ring. The transformation of crystal molecule sequence arrangement to the amorphous form causes peak broadening or peak change.³³ In F2 and F5, the β -lactam $\nu\text{C}=\text{O}$ was shifted toward lower frequencies of 1734 and 1751 cm^{-1} . The carboxylate νCOO^- (1587 cm^{-1}) and νCOO^- (1359 cm^{-1}) were shifted toward higher frequencies (1598 cm^{-1}) and (1381 cm^{-1}), respectively, after making a SD of AM. For F5, carboxylate νCOO^- (1587 cm^{-1}) and νCOO^- (1359 cm^{-1}) shifted toward lower frequencies (1512 cm^{-1}) and (1255 cm^{-1}), respectively. This minor shift is because the drug has some H-bonding with the polymers.

It is also evident that there is no chemical interaction between the drug and polymers as all the vital signs of polymer

and drug are detectable in the spectra. The results revealed no considerable changes in the IR peaks of AM in the prepared SDs compared to that of the pure drug, indicating no interaction.

2.5.2. Scanning Electron Microscopy. Scanning electron microscopy (SEM) examination of both polymers resulted in different morphologies. HP- β -CD appeared as a spherical-shaped, smooth-surfaced polymer having several crevices in its structure. HPMC exhibited irregular-shaped, rough-surfaced, large-sized particles. Both the polymers were amorphous in nature, as shown in Figure 6. These SEM images of HP- β -CD and HPMC agreed with the research results described by Li et al. (2016) and Novák et al. (2012).^{34,35} AM appeared as a flat rod-shaped crystal, as presented in Figure 3. Our observations were comparable to those of Songsurang et al. (2010).³⁶

Morphological differences observed in the structure of the drug and SDs were obvious. The SEM images showed that the

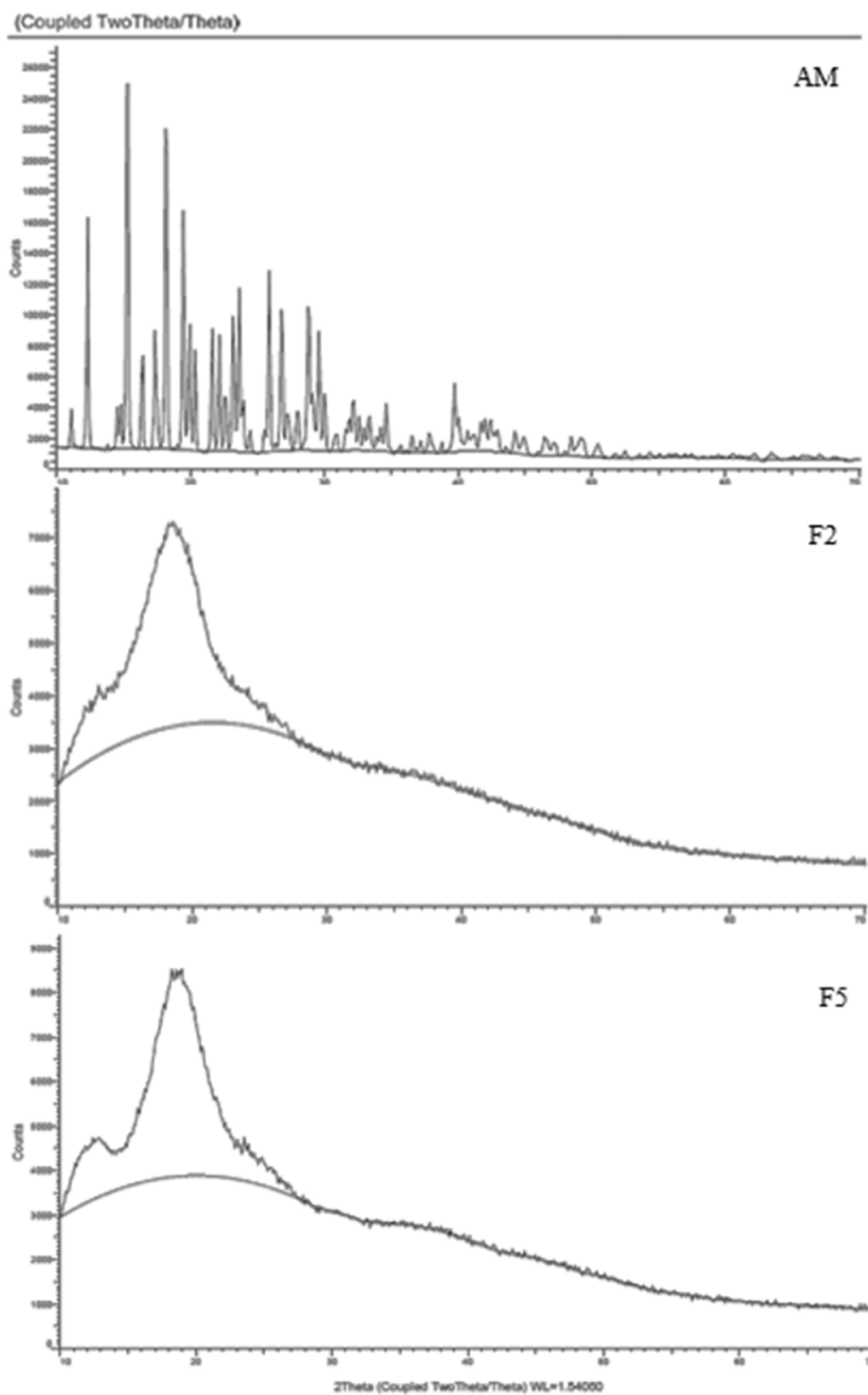


Figure 5. PXRD patterns of AM, F2, and F5.

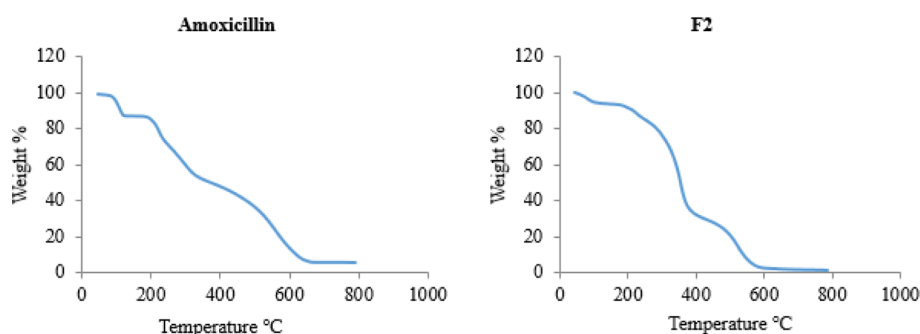


Figure 6. Thermogravimetric curve of AM and F2.

crystalline morphology of AM was transformed into amorphous biconcave discoid-shaped particles (F2 and F5). This behavior might be attributed to the quick process of spray drying. The SDs appeared as amorphous shriveled-shaped particles with enhanced surface area. Harsha (2013) also observed similar findings and attributed this behavior as beneficial for enhancing the dissolution rate.³⁷ During the spray drying process, the structure of the drug and polymers were modified into SDs as a result of the high temperature, pressure, and fast evaporation rate of the solvent. SEM studies of all the SDs confirmed that drug particles were distributed in the polymeric matrix to develop amorphous structures. The modifications observed by SEM analysis were also justified by DSC studies.

2.5.3. Powder X-ray Diffraction. A powder X-ray diffraction (PXRD) study was carried out to determine the crystallinity of the newly developed spray-dried SDs. The number of peaks represents the level of crystallinity in a sample. The XRD patterns of HP- β -CD and HPMC show the amorphous nature of the polymers (Figure 4). The graphs for the standard AM showed a number of peaks, proving that the drugs were crystalline. The PXRD patterns of SDs (F1–F6) showed that as the quantity of the polymer in the SD increases, some very low-intensity peaks for drugs were seen. F1 and F4 consisted of 50% drug and 50% polymer (1:1) and showed some crystallinity for AM, suggesting that the entire drug might not be present in its amorphous form. F2 and F5 (Figure 5) and F3 and F6, made with 33.3% drug and 66.6% polymer (1:2) and 25% drug and 75% polymer (1:3), respectively, showed an amorphous nature for a SD, suggesting that the drug present might be in its amorphous form. The formation of an amorphous state proves that the drug was dispersed in a molecular state with HP- β -CD and HPMC.

Alam et al. (2012) stated that the drug–polymer ratio is an important factor in controlling the nature of the phase of the SD. The SD will result as crystalline if the ratio of the constituent drug is higher than that of the polymer.³⁸ Therefore, the crystallization rate can be retarded to some extent by increasing the ratio of polymer.³⁹ Consequently, the solubility and release rate can be improved.

2.5.4. Thermal Analysis. The effect of polymers was analyzed on the thermal stability of AM and its SDs (1:2) by TGA. The three-step degradation pattern of each sample was determined by an overlay of TG and DTG curves, and the temperature range selected for the study was 0–800 °C. AM was decomposed in a single step.

The thermal degradation of AM was carried out in three steps. During the first step, the initial thermal decomposition temperature (T_{d_i}) of AM was recorded to be 91 °C, the final

decomposition temperature (T_{d_f}) was calculated as 120 °C, and the maximum temperature (T_{d_m}) of AM was calculated as 108 °C. The weight loss of the standard AM was calculated to be 87.76%. The initial temperature value during the second step was determined as 202 °C, the final temperature of the standard AM was recorded as 324 °C, and the maximum temperature was 259 °C. The loss of the total weight of the sample was determined as 54.82%. During the third step, the initial thermal decomposition temperature (T_{d_i}) of AM was recorded to be 504 °C, the final decomposition temperature (T_{d_f}) was calculated as 635 °C, and the maximum temperature (T_{d_m}) of AM was calculated as 564 °C. The weight loss of the standard AM was calculated to be 7.65%. The char yield value of AM was found to be 68.9% after complete degradation at 600 °C. The degradation pattern of AM is shown in Figure 6. Degradation parameters are given in Table 3.

Table 3. Average Thermal Decomposition Temperatures, Weight Loss %, and Char Yield of AM and F1–F3

sample	step	T_i (°C)	T_m (°C)	T_f (°C)	weight loss % at T_f	char yield wt (%)
AM	I	91	108	120	87.76	68.9 at 600 °C
	II	202	259	324	54.82	
	III	504	564	635	7.65	
F1	I	260	320	373	41.50	44.82 at 600 °C
	II	451	511	553	8.47	
F2	I	295	338	375	37.67	45.81 at 600 °C
	II	488	510	546	8.85	
F3	I	330	360	402	29.09	36.71 at 600 °C
	II	487	524	558	6.18	

The thermal degradation temperature of the three SDs composed of different ratios AM and HP- β -CD (F1–F3) was carried out in two steps. During the first step, the initial thermal decomposition temperature (T_{d_i}) of F1 was recorded to be 260 °C, the final decomposition temperature (T_{d_f}) was calculated as 373 °C, and the maximum temperature (T_{d_m}) of AM was calculated as 320 °C. The weight loss of the SDs was calculated to be 41.50%. The initial temperature during the second step was determined as 451 °C, the final temperature of SDs was recorded as 553 °C, and the maximum temperature was 511 °C. The loss of the total weight of the sample was determined as 8.47%. The char yield of F1 was found to be 44.82% after complete degradation at 600 °C.

During the first step, the initial thermal decomposition temperature (T_{d_i}) of F2 was recorded to be 295 °C, the final

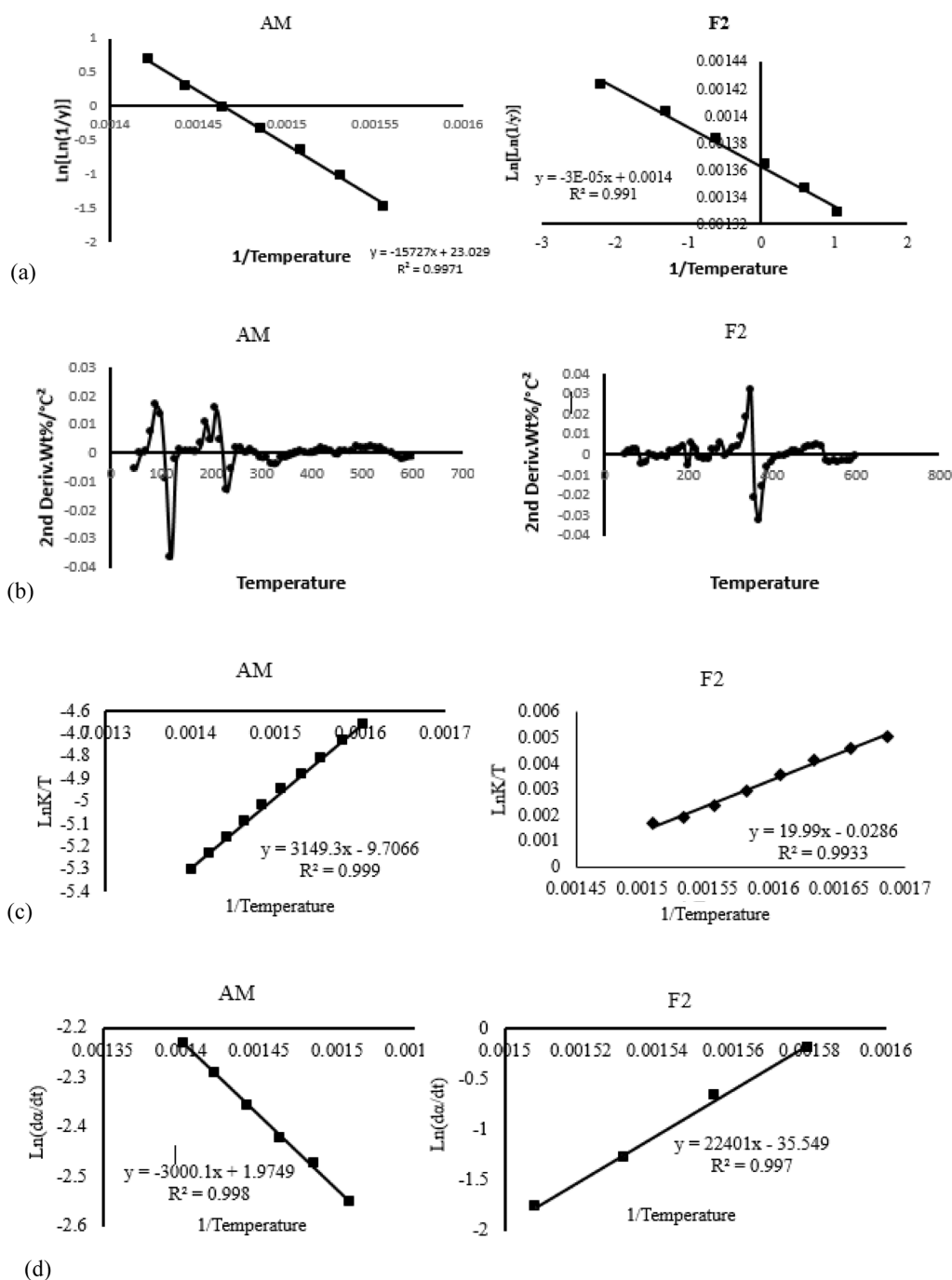


Figure 7. (a) Broidi analysis of AM and F2. (b) Kissinger analysis of AM and F2. (c) Eyring–Polanyi analysis of AM and F2. (d) Friedman analysis of AM and F2.

decomposition temperature (T_{d_i}) was calculated as 375 °C, and the maximum temperature (T_{d_m}) of AM was calculated as 338 °C. The weight loss of the SDs was calculated to be 37.67%. The initial temperature during the second step was determined as 488 °C, the final temperature of the SDs was recorded as 546 °C, and the value of the maximum temperature was 510 °C. The loss of the total weight of the sample was determined as 8.85%. The char yield value of F2 was found to be 45.81% after complete degradation at 600 °C.

During the first step, the initial thermal decomposition temperature (T_{d_i}) of F3 was recorded to be 330 °C, the final decomposition temperature (T_{d_f}) was calculated as 402 °C, and the maximum temperature (T_{d_m}) of AM was calculated as

360 °C. The weight loss of the pure sample was calculated to be 29.09%. The initial temperature during the second step was determined as 487 °C, the final temperature of SDs was recorded as 558 °C, and the maximum temperature was 524 °C. The loss of the total weight of the sample was determined as 6.18%. The char yield value of F3 was 36.71% after complete degradation at 600 °C. Kinetic models were applied, and the results are shown in Figure 7a–d.

2.5.5. In Vitro Dissolution Study. Dissolution profiles of market-available tablets of AM (Augmentin), and tablets based on spray-dried amorphous SDs of AM T1–T6 in two different buffers, pH 1.2 and 6.8, are shown in Figure 8a–d. At pH 1.2 and 6.8, T1–T6 have shown a lower rate of dissolution than

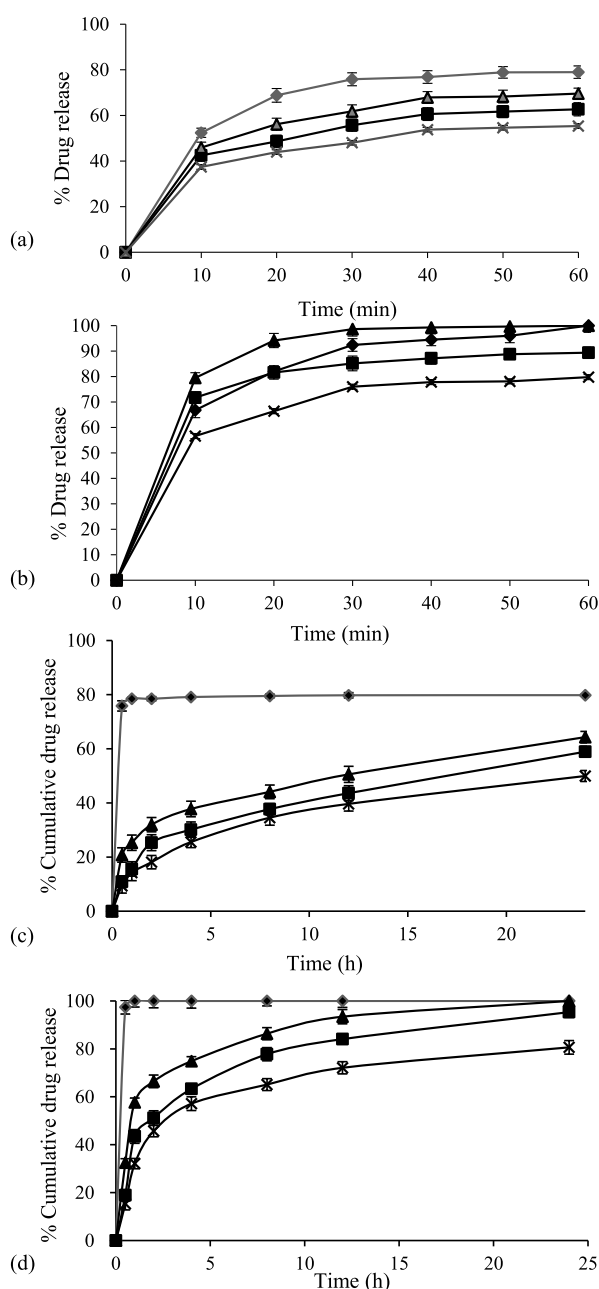


Figure 8. (a) Cumulative % drug release of Augmentin (◆), T1 (■), T2 (▲), and T3 (×) at pH = 1.2. Values are expressed as mean \pm SE ($n = 3$). (b) Cumulative % drug release of Augmentin (◆), T1 (■), T2 (▲), and T3 (×) at pH 6.8. Values are expressed as mean \pm SE ($n = 3$). (c) Cumulative % drug release of Augmentin (◆), T4 (■), T5 (▲), and T6 (×) at pH 1.2. Values are expressed as mean \pm SE ($n = 3$). (d) Cumulative % drug release of Augmentin (◆), T4 (■), T5 (▲), and T6 (×) at pH 6.8. Values are expressed as mean \pm SE ($n = 3$).

that of market-available Augmentin. The *in vitro* dissolution study of all tablets, T1–T6, showed sustained drug release at pH 6.8. Among the prepared tablets, tablets based on SDs 1:2 showed the most sustained release profile. Dissolution of the spray-dried SDs presented an excipient-dependent profile. Increasing the polymer concentration increases the viscosity via physical entanglement, consequently retarding the drug diffusion and release from the polymeric matrix. Comparing both polymeric carriers, the tablets based on HPMC showed a

sustained release profile, whereas HP- β -CD displayed an immediate release profile. This indicated that spray drying technology is highly efficient in preparing sustained-release products.

Among the tablets T1–T3, T2 showed the best release profile. The results confirmed that the rate of drug release depends upon the concentration of the drug. During the dissolution process, the tablet disintegrates, reducing the surface area with time (Table 4). This concept is related to the diffusion process.⁴⁰

The SDs of AM with different ratios of HPMC (1:1, 1:2, and 1:3) have sustained release. However, the observed sustained release rate of AM was also dependent on the ratio of the polymer. Among the tablets T4–T6, the best release profile was displayed by T5 (1:2). The best linearity was found in the first-order model for Augmentin ($R^2 = 1$ at pH 1.2 and 6.8) and T5 ($R^2 = 0.996$ and 0.971 at pH 1.2 and 6.8, respectively). This indicates that drug release depended on the concentration (Table 4 and Figure 9).

The postcompression properties of the tablets (T1–T6) based on the SD of AM (F1–F6) are presented in Table 5. The standard calibration curve of AM in a 0.1 N HCl buffer solution was a straight line with a regression coefficient of 0.998. Content uniformity of all the batches was observed from 94.78 to 99.21%, with a standard deviation of less than 8% within the range of USP30-NF27 (2007). Uniformity in weight designates the equivalent size and particle distribution within the compressed tablets. Friability values were less than 1%, meeting the official United States Pharmacopeia (USP) requirements. Since friability was less than 1%, compressed tablets possessed good mechanical strength and could tolerate obtainable stress throughout packaging and transportation. The hardness values were in the range of 4.19–5.76 kg/cm², describing excellent mechanical strength.

2.5.6. In Vivo Drug Release. The validated HPLC method was used to analyze the rabbit plasma samples obtained at various sampling times after oral administration of AM, T2, and T5. The *in vivo* drug release profiles of Augmentin and tablets based on spray-dried amorphous SD of AM, T2, and T5 in blood plasma are shown in Figure 10. T2 and T5 tablets have shown a higher dissolution rate than market-available Augmentin. The mean plasma concentration–time curves of AM tablets T2 and T5 after a single oral dose of 7.14 mg kg⁻¹ are shown in Figure 10. Following oral administration, the peak serum concentration of the AM occurred at 2 h with a C_{max} of 281 mg mL⁻¹ (Table 6).

The plasma concentration versus time curve displayed the delayed release of T5 compared to that of Augmentin and T2. The C_{max} value of Augmentin, T2, and T5 was 281, 405.26, and 391.76 μ g mL⁻¹, respectively. The higher value of C_{max} for the prepared tablets indicated the benefit of the low dose frequency. The time to reach the maximum concentration of AM in plasma was 2, 2, and 4 h for Augmentin, T2, and T5, respectively. The half-life ($t_{1/2}$) achieved for Augmentin, T2, and T5 was 10.37, 12.03, and 20.06 h, respectively. The longer value of $t_{1/2}$ confirmed the sustained drug release from SD-based tablets. Spray-dried SD F2 and F5-based tablets T2 and T5 showed better drug release profiles than Augmentin. The absorption of spray-dried SDs into the systemic circulation via the intraperitoneal route was, therefore, rapid and high. The value of the area under the curve (AUC) of T2 and T5 was 2473.79 and 1973.03 h· μ g mL⁻¹, respectively, was greater than that of Augmentin (1490.42 h· μ g mL⁻¹). Larger values of AUC

Table 4. Release Kinetic Parameters for Augmentin and T5 at pH = 1.2 and 6.8

kinetic model	rate constants	formulations			
		pH = 1.2		pH = 6.8	
		Augmentin	T5	Augmentin	T5
zero-order	K_0 (% h ⁻¹)	1.163	3.012	2.078	1.391
	R^2	0.118	0.543	0.753	0.105
first-order	K_1 (% h ⁻¹)	0.012	0.009	0.01	0.015
	R^2	1	0.996	1	0.971
second-order	K_2 (% h ⁻¹)	0.011	0.050	0.050	0.025
	R^2	0.144	0.309	0.309	0.1
Higuchi	K_H (% h ^{-1/2})	11.37	18.62	9.319	11.80
	R^2	0.799	0.834	0.291	0.935
Hixson–Crowell	K_{HC} (% h ⁻¹)	0.029	0.255	0.255	0.097
	R^2	0.133	0.49	0.491	0.103

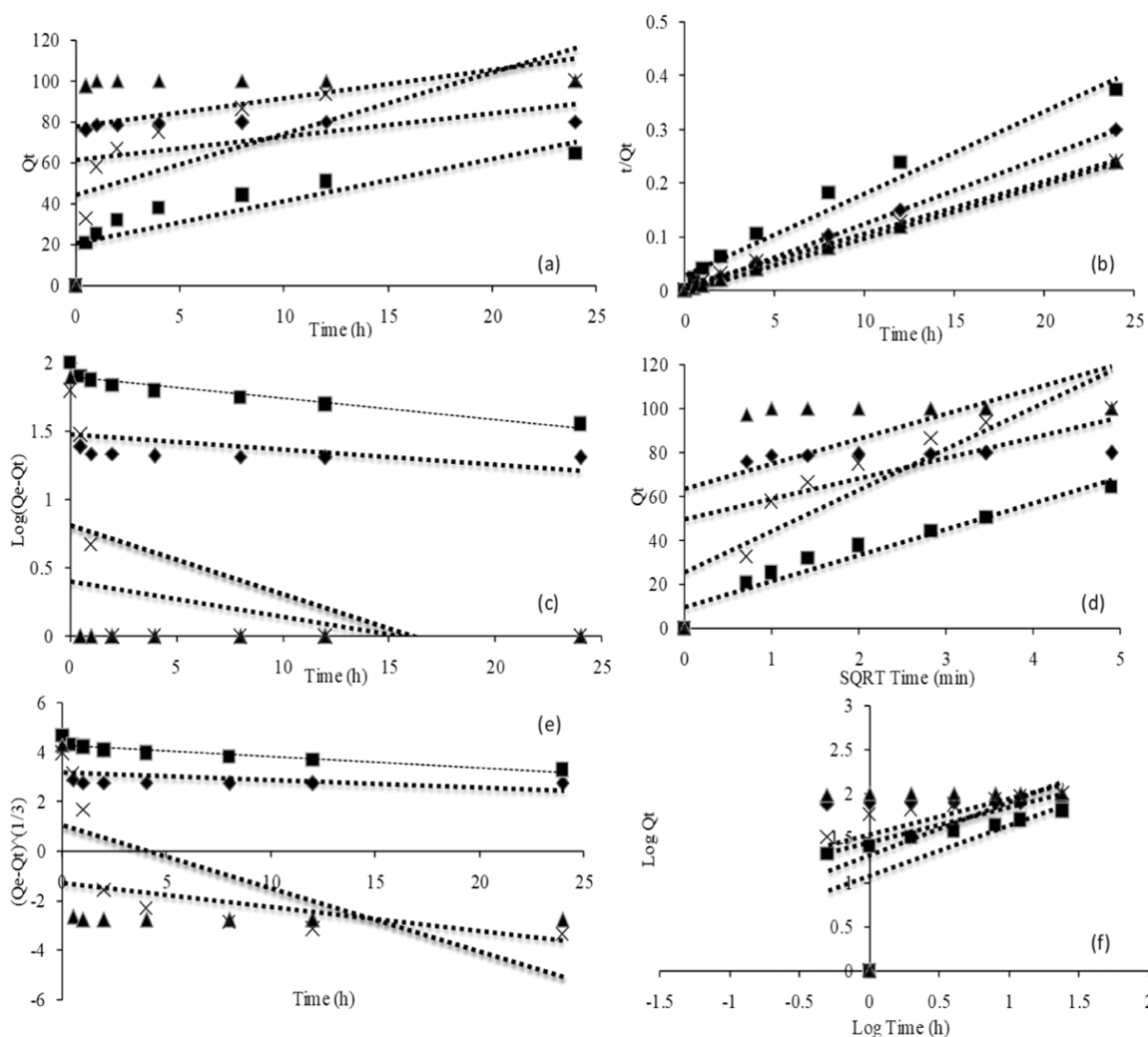


Figure 9. Drug release kinetics of Augmentin at pH 1.2 (◆) and pH 6.8 (■) and that of T5 at pH 1.2 (▲) and pH 6.8 (×): (a) zero-order kinetics, (b) first-order kinetics, (c) second-order kinetics, (d) Higuchi kinetics, (e) Hixson–Crowell kinetics, and (f) Korsmeyer–Peppas kinetics.

indicated the enhanced bioavailability of the newly developed tablets. Enhanced bioavailability is of great therapeutic importance, such as lower side effects and price.

3. CONCLUSIONS

The current study concludes that SD powder formulations of AM using varied ratios of HP- β -CD (F1–F3; 1:1–1:3) and HPMC (F4–F6; 1:1–1:3) prepared by the spray drying

technique were fine, spherical, stable particles. The formulations were highly soluble in water. The SD powders (F1–F6) and tablets (T1–T6) were found within official limits with respect to pre- and postcompression parameters, respectively. *In vitro* and *in vivo* dissolution studies confirmed better drug release and pharmacokinetic parameters than market-available Augmentin. Among the formulations, F2 and F5, with a ratio of 1:2 of polymers, showed the best properties for all the

Table 5. Postcompression Properties of Tablets T1–T6

tablet	postcompression properties					
	DC uniformity %	weight variation (mg)	friability %	hardness (kg/cm ²)	thickness (mm)	diameter (mm)
T1	98	265 ± 1.54	0.474 ± 0.04	4.19 ± 0.34	4.21 ± 0.03	8.23 ± 0.01
T2	97.86	390 ± 1.98	0.334 ± 0.03	5.62 ± 0.12	5.23 ± 0.04	8.65 ± 0.01
T3	94.84	515 ± 1.43	0.483 ± 0.15	5.87 ± 0.85	4.11 ± 0.01	8.71 ± 0.04
T4	99.21	265 ± 1.63	0.655 ± 0.10	5.90 ± 0.26	4.32 ± 0.05	8.44 ± 0.09
T5	96.66	390 ± 0.98	0.529 ± 0.02	5.41 ± 0.98	5.37 ± 0.06	8.31 ± 0.02
T6	94.78	515 ± 1.55	0.545 ± 0.32	5.76 ± 0.41	5.26 ± 0.08	8.55 ± 0.01

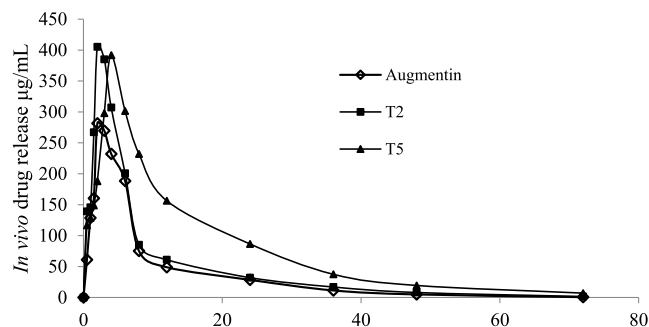


Figure 10. Mean plasma concentration–time profile of Augmentin (◆), T2 (▲), and T5 (■).

Table 6. Pharmacokinetic Analysis of Augmentin, T2, and T5

parameters	Augmentin	T2	T11
C_0 (µg/mL)	107.89	135.51	132.73
K (h ⁻¹)	0.066	0.057	0.034
V_d (L)	0.06524	0.06515	0.07584
$t_{1/2}$ (h)	10.37	12.03	20.06
clearance (Lt ^{1/2})	0.0043	0.0037	0.0026
C_{max} (µg/mL)	281	405.26	391.76
T_{max} (h)	2	2	4
AUC (h·µg/mL)	1490.42	2473.79	1937.03

parameters studied. F5 (AM/HPMC = 1:2) had better-sustained release properties than F2 (AM/HP-β-CD).

4. MATERIALS AND METHODS

4.1. Materials. Standard antibiotic AM was acquired from StandPharm Pakistan (Pvt.) Ltd., Lahore, Pakistan. The water-soluble polymeric carriers hydroxypropyl β CD (HP-β-CD) and HPMC were purchased from Sigma-Aldrich (Germany) via the local market. Analytical-grade reagents and solvents such as methanol, ethanol, acetone, sodium hydroxide (NaOH), hydrochloric acid (HCl), potassium bromide, microcrystalline cellulose, and magnesium stearate were purchased from Sigma-Aldrich. HPLC mobile-phase solvents such as methanol, acetonitrile, phosphoric acid, and acetic acid were purchased from Merck. Purified water was prepared by the reverse osmosis technique.

4.2. Methods. **4.2.1. Preparation of SDs.** Six different SDs F1–F6 consisting of different ratios of the drug and polymer were prepared by the spray drying technique. The compositions of SDs are presented in Table 7. AM was dissolved in methanol (7.5 mg mL⁻¹) to prepare the drug solution. The polymer was dissolved in water (500 mg mL⁻¹) to prepare an aqueous polymer solution. The drug solution and aqueous solution of the polymer were mixed and stirred for 30 min at 1500 rpm to prepare a homogeneous solution of

Table 7. Composition of SDs F1–F6

SDs	AM (g)	HP-β-CD (g)	HPMC (g)	drug–polymer ratio
F1	5	5		1:1
F2	3.3	6.6		1:2
F3	2.5	7.5		1:3
F4	5		5	1:1
F5	3.3		6.6	1:2
F6	2.5		7.5	1:3

the drug and polymer. The solutions were spray-dried using a laboratory-scale spray dryer (Pilotech) under the conditions shown in Table 8. Finally, SDs were collected.

Table 8. Conditions Set for the Spray Drying Process

	parameters	F1–F3	F4–F6
1	inlet temperature (°C)	120	128
2	outlet temperature (°C)	30.3	48.4
3	oxygen concentration, mPa	1.30	1.45
4	condensation temperature (°C)	70.4	89.5
5	feed pump rate (rpm)	35	35
6	air blower frequency (Hz)	38	38

4.2.2. Preliminary Studies of SDs. Preliminary studies included the determination of PY and the percent DC of the newly prepared SDs. The PY of all SDs was determined by applying the following equation

$$PY = \text{actual weight of SD} \times 100 / \text{theoretical weight of SD}$$

The DC of all SDs was calculated using a PharmaSpec UV-1700 spectrophotometer (Shimadzu, Japan). Solutions of the drug and SDs F1–F6 were prepared as follows: samples equivalent to 50 mg of the drug were weighed accurately and dissolved in 50 mL of a suitable solvent. The solutions were stirred for 24 h, filtered, and scanned at 275 nm. Percent DC (%DC) was calculated by applying the following⁴¹

$$\%DC = \text{mass of entrapped drug} \times 100 / \text{mass of SD}$$

4.2.3. Flow Properties. Flow properties of drug and SD powders F1–F6 were analyzed by measuring the following parameters using USP Method I.⁴² The AOR of samples was measured by the funnel method. SD powder was allowed to flow through the funnel. The cone height and diameter of dropped powder were measured. The AOR (θ) was determined by applying the equation below

$$\alpha = \tan^{-1} h/r$$

The sample (4 g) was added to a 50 mL graduated cylinder, and the bulk volume was measured. Bulk density was calculated by applying the following equation

$$\text{bulk density } (d_b) = M/V_0$$

The cylinder was tapped at a height of 20 mm at the rate of 100 drops. The final volume (tapped volume, V_f) was determined to calculate the tapped density using the equation as follows

$$\text{tapped density } (d_T) = M/V_f$$

Hausner's ratio and Carr's compressibility index⁴³ of samples were calculated using bulk density and tapped density by equations given below

$$\text{Hausner's ratio} = V_0/V_f$$

$$\text{Carr's compressibility index (CI)} = 100 \times (V_0 - V_f)/V_0$$

where M is the powder mass, V_0 is the initial powder volume, and V_f is the final powder volume after 100 tapings.

4.2.4. Solubility Study. The solubility of AM and the SDs F1–F6 in distilled water and buffers of pH 1.2 and 6.8 was determined using a spectrophotometer (UV-1700, Shimadzu, Japan). For this purpose, solutions of each sample were prepared by stirring an excess drug in water and buffers for at least 24 h at the ambient temperature (25 °C) at 200 rpm. Subsequently, supersaturated solutions were filtered (pore size 0.22 μm) and diluted for the measurements. The solubility of samples in aqueous and buffer mediums was determined by noting the absorbance at their respective 275 nm. Finally, drug amounts were calculated by corresponding calibrations.

4.3. Characterization. **4.3.1. Fourier Transform Infrared Spectroscopy.** The FTIR spectra of the standard, polymer, and all formulations were obtained using an FTIR spectrometer (IR-Prestige 21, Shimadzu, Japan) after appropriate background subtraction. A homogeneous mixture of the sample (1 mg) and dry potassium bromide (10 mg) was compressed into transparent pellets.⁴⁴ The pellets were scanned from 4000 to 400 cm^{-1} .⁴⁵

4.3.2. PXRD Study. PXRD patterns of standard and the six SDs were recorded using a Bruker D8 Discover X-ray diffractometer to determine their amorphous or crystalline nature. The finely divided powder samples were placed on a sample slide and scanned. The instrument was operated at 25 mA and a voltage of 40 kV at a scanning range of $5 < 2\theta < 40^\circ$ at 2° min^{-1} . In the characteristic diffraction pattern of each sample, the position of the peak indicated the lattice spacing.²⁵

4.3.3. Thermogravimetric Analysis and Thermal Kinetics. Thermogravimetric analysis of the drug and SDs F1–F6 was performed using simultaneous thermal analyzer SDT Q600 (TA Instruments, USA). Thermal degradation of each sample was recorded in the temperature range of ambient to 800 °C with nitrogen purging at 100 mL min^{-1} . The thermal data was processed using Universal Analysis 2000 v 4.2E software (TA Instruments, USA). Thermogravimetric data was analyzed by different thermal kinetic methods.²⁸

4.3.4. Scanning Electron Microscopy. The surface morphology of AM and its SDs (F1–F6) was analyzed by SEM. Each sample was placed on a conductive carbon tape attached to sample stubs and then coated with a Au–Pd alloy (60:40) in a Cressington 208 HR Sputter Coater. Samples of each drug, polymer, and SDs were scanned using a high-performance LEO (Zeiss) 1550 Schottky field emission SEM system equipped with a Gemini lens and capable of resolution in a 2–5 nm size range. The images were captured at different

magnifications using the latest version of Smart SEM V05.03.00 software.⁴⁶

4.3.5. Tablet Compression. The SDs F1–F6 were compressed into the tablets T1–T6 using a ZP-19 rotary press under a 15 kN force with 7 mm round flat punches. Each batch (F1–F6) contained 20 tablets. The SD equivalent to 125 mg of the drug was mixed with MCC (Microcrystalline Cellulose) and Mg stearate in a polythene bag (6 × 9 cm). The composition of each tablet is given in Table 9.

Table 9. Composition of Tablets from Batch T1–T6

tablets	composition (mg)			total mass (mg)
	SD	MCC	Mg stearate	
T1	250	5	10	265
T2	375	5	10	390
T3	500	5	10	515
T4	250	5	10	265
T5	375	5	10	390
T6	500	5	10	515

4.3.6. Postcompression Properties. After noting the mean weight of 20 tablets from each batch (T1–T6), the tablets were crushed to get a fine powder. Powder equivalent to 10 mg of the drug was accurately weighed and dissolved in water. The solution was filtered, diluted, and scanned at 275 nm using a UV/visible spectrophotometer. Therefore, the DC, standard deviation, and % relative standard deviation of all the tablets (T1 to T6) were noted. Twenty tablets from each batch were weighed accurately. The mean weight was compared to the individual weight of each tablet to determine the weight variation. Six tablets were randomly selected from each batch of SD formulations, dedusted, weighed accurately, and kept in a friabilator (Roche Friabilator). A rotating drum was preset at 25 rpm, and the tablets were dropped down from a height of 6 inches. After completing 100 rotations, tablets were withdrawn from the friabilator, dedusted, and weighed accurately. Afterward, these tablets were tested for hardness, thickness, and diameter using a hardness tester. The standard deviation of all the formulations was calculated, and every measurement was done in triplicate. Crushing strength data, diameter, and thickness values were used to measure the tensile strength of all the formulations. Each measurement was recorded in triplicate to get accurate results.³¹

4.3.7. In Vitro Dissolution Study. The *in vitro* drug release study of tablets T1–T6 and market-available Augmentin, 125 mg, was carried out using a USP paddle apparatus (Pharma test PT-DT 7, Germany) following the standard method given in USP 2011. The dissolution apparatus media was set at 37 ± 0.5 °C at 100 revolutions per minute (rpm). Drug release was studied at pH 1.2 and pH 6.8 for 1 h. An aliquot (5 mL) was drawn from the dissolution medium at 10, 20, 30, 40, 50, and 60 min and was replaced with the same quantity of buffer to maintain the level constant. For the SDs composed of HPMC, the study was further extended to 24 h. An aliquot (5 mL) was drawn from the dissolution medium at 1, 2, 4, 6, 12, and 24 h and was replaced with the same quantity of buffer to maintain the level constant. Absorbance was measured using a UV/vis spectrophotometer (UV-1700 Shimadzu, Germany) at 275 nm. Cumulative percent release at various time periods was calculated.

4.3.8. Pharmacokinetic Study. The developed HPLC method was applied to analyze and compare the pharmaco-

kinetic parameters of market-available Augmentin and SD-based tablets (T2 and T5). The study was approved by the Biosafety and Ethical Review Committee, University of Sargodha (approval letter no. SU/ORIC/2544). Six white albino rabbits of either sex (body weight ~ 1.5 kg) were obtained from the Laboratory Animal House at the University of Sargodha, Sargodha, Pakistan. The animals were kept in cages and acclimatized under a 12 h light/dark cycle. These animals were fasted for 10 h (overnight) and were stopped from taking water 1 h prior to dose administration. Animals were randomized into three groups. Each group consisted of three rabbits.

GI: Rabbits treated with oral tablets of Augmentin (7.14 mg kg^{-1})

G II: Rabbits treated with T2 (7.14 mg kg^{-1})

G III: Rabbits treated with T5 (7.14 mg kg^{-1})

After 10 min of drug administration, the animals were provided with standard food and water throughout the trial of 24 h. After dosing, blood samples (3 mL) were collected from the jugular vein of each rabbit at 0, 0.5, 1, 2, 4, 6, and 8 h into heparin tubes (Leo, Denmark).⁴⁷ Samples were centrifuged at 6000g for 5 min. Plasma samples were separated by taking a supernatant layer and accumulated in capped test tubes sealed with aluminum foil and labeled accordingly. The plasma samples were stored at -5 °C in a freezer (PEL FR-320) until analysis. Each plasma sample was thawed and added with acetonitrile (0.5 mL), acetic acid (0.5 mL), and a few drops of *o*-phosphoric acid. These vials were incubated for 15 min to precipitate soluble plasma proteins. To obtain plasma, each vial containing precipitated proteins was centrifuged at 6000g for 10 min. As a result, a clear supernatant was collected and filtered using nylon syringe filters (0.45 μm). Therefore, the samples were ready for HPLC/UV analysis.

4.3.9. High-Performance Liquid Chromatography. HPLC analysis was carried out using a mobile phase composed of methanol: water (35:65, v/v) with an injection volume of 20 μL and a flow rate of 1 mL min^{-1} at a column temperature of 25 °C (10 min run time, 4.66 min retention time, and 272 nm λ_{max}).⁴⁸ The drug quantity in each plasma sample was determined from the peak area observed in the respective chromatogram. Concentration–time curves were plotted using Microsoft Excel 2010 and analyzed by the linear trapezoidal method. Various pharmacokinetic parameters, such as AUC_{0-t} , $\text{AUC}_{0-\infty}$, C_{max} , T_{max} , $t_{1/2}$, V_d , and Cl , were calculated. K_e was determined by the regression analysis of at least three data points in the terminal phase.

We thankfully acknowledge the financial support of the Higher Education Commission (HEC) of Pakistan under the NRPU Project, HEC-NRPU Project no. 20-4007/NRPU/R&D/HEC/14/248.

AUTHOR INFORMATION

Corresponding Authors

Muhammad Sher – Institute of Chemistry, University of Sargodha, Sargodha 40100, Pakistan; Email: msherawan@yahoo.com

Muhammad Fayyaz ur Rehman – Institute of Chemistry, University of Sargodha, Sargodha 40100, Pakistan; orcid.org/0000-0003-2901-7212; Email: fayyaz9@gmail.com

Huibiao Deng – Department of Critical Care Medicine, Shanghai General Hospital, Shanghai Jiao Tong University

School of Medicine, Shanghai 200127, China;

Email: shengmideng@163.com

Authors

Faiza Hassan – Institute of Chemistry, University of Sargodha, Sargodha 40100, Pakistan

Muhammad Ajaz Hussain – School of Chemistry, University of the Punjab, Lahore 54600, Pakistan; orcid.org/0000-0003-4570-6616

Mubshara Saadia – Department of Chemistry, Ghazi University, Dera Ghazi Khan 32200, Pakistan

Muhammad Naeem-Ul-Hassan – Institute of Chemistry, University of Sargodha, Sargodha 40100, Pakistan

Muhammad Tahir Haseeb – College of Pharmacy, University of Sargodha, Sargodha 40100, Pakistan; orcid.org/0000-0002-1883-7226

Syed Nasir Abbas Bukhari – Department of Pharmaceutical Chemistry, College of Pharmacy, Jouf University, Sakaka, Aliouf 2014, Saudi Arabia

Azhar Abbas – Institute of Chemistry, University of Sargodha, Sargodha 40100, Pakistan; Department of Cardiothoracic Surgery, The Second Affiliated Hospital of Guangzhou University of Chinese Medicine, Guangzhou, Guangdong 510006, China

Bo Peng – Government Ambala Muslim Graduate College, Sargodha 40100, Pakistan

Fariha Kanwal – School of Biomedical Engineering and Med-X Research Institute, Shanghai Jiao Tong University, Shanghai 201620, China

Complete contact information is available at:

<https://pubs.acs.org/10.1021/acsomega.2c06662>

Notes

The authors declare no competing financial interest.

ACKNOWLEDGMENTS

We are thankful to Dr. Rujie Cai for their help and support.

REFERENCES

- (1) Gordon, R. C.; Regamey, C.; Kirby, W. M. Comparative clinical pharmacology of amoxicillin and ampicillin administered orally. *Antimicrob. Agents Chemother.* **1972**, *1*, 504–507.
- (2) Kaur, S. P.; Rao, R.; Nanda, S. Amoxicillin: a broad spectrum antibiotic. *Int. J. Pharm. Biol. Sci.* **2011**, *3*, 30–37.
- (3) El-Nahhal, Y.; El-Dahdouh, N. Toxicity of amoxicillin and erythromycin to fish and mosquito. *Ecotoxicol. Environ. Saf.* **2015**, *10*, 13–21.
- (4) Zango, U. U.; Ibrahim, M.; Shawai, S. A. A.; Shamsuddin, I. M. A review on β -lactam antibiotic drug resistance. *MOJ drug des. dev. ther.* **2019**, *3*, 52–58.
- (5) Navarro, A. S. New formulations of amoxicillin/clavulanic acid. *Clin. Pharmacokinet.* **2005**, *44*, 1097–1115.
- (6) Gresser, U. Amoxicillin-clavulanic acid therapy may be associated with severe side effects—review of the literature. *Eur. J. Med. Res.* **2001**, *6*, 139–149.
- (7) Garbutt, J. M.; Banister, C.; Spitznagel, E.; Piccirillo, J. F. Amoxicillin for Acute Rhinosinusitis. *J. Am. Med. Assoc.* **2012**, *307*, 685–692.
- (8) Tucker, M. H.; Lomas, C. M.; Ramchandrar, N.; Waldram, J. D. Amoxicillin challenge without penicillin skin testing in evaluation of penicillin allergy in a cohort of Marine recruits. *J. Allergy Clin. Immunol.* **2017**, *5*, 813–815.
- (9) Jacobson, G. F.; Autry, A. M.; Kirby, R. S.; Liverman, E. M.; Motley, R. U. A randomized controlled trial comparing amoxicillin

and azithromycin for the treatment of Chlamydia trachomatis in pregnancy. *Am. J. Obstet. Gynecol.* **2001**, *184*, 1352–1356.

(10) Martinot, J.-B.; Carr, W.; Carr, S.; Cullen, J. L. H.; Budo, K.; Bauer, C.; MacLeod, C. M.; Sanguinetti, W. C.; van Veldhuizen, W. C. J. A comparative study of clarithromycin modified release and amoxicillin/ clavulanic acid in the treatment of acute exacerbation of chronic bronchitis. *Adv. Ther.* **2001**, *18*, 1–11.

(11) Butler, T. The Jarisch-Herxheimer Reaction After Antibiotic Treatment of Spirochetal Infections: A Review of Recent Cases and Our Understanding of Pathogenesis. *Am. J. Trop. Med. Hyg.* **2017**, *96*, 46.

(12) Cundiff, J.; Joe, S. Amoxicillin-clavulanic acid-induced hepatitis. *Am. J. Otolaryngol.* **2007**, *28*, 28–30.

(13) Rolinson, G. N. Laboratory evaluation of amoxicillin. *J. Infect. Dis.* **1974**, *129*, S139–S145.

(14) Hörter, D.; Dressman, J. Influence of physicochemical properties on the dissolution of drugs in the gastrointestinal tract. *Adv. Drug Deliv. Rev.* **2001**, *46*, 75–87.

(15) Ghumman, S. A.; Mahmood, A.; Noreen, S.; Rana, M.; Hameed, H.; Ijaz, B.; Hasan, S.; Aslam, A.; ur Rehman, M. F. Formulation and evaluation of quince seeds mucilage–sodium alginate microspheres for sustained delivery of cefixime and its toxicological studies. *Arab. J. Chem.* **2022**, *15*, 103811.

(16) Ullah, F.; Ali Khan, M. F.; Khan, N. H.; Rehman, M. F.; Shah, S. S.; Mustaqeem, M.; Ullah, S.; Zhang, Q.; Shi, H. Simvastatin-Loaded Lipid Emulsion Nanoparticles: Characterizations and Applications. *ACS Omega* **2022**, *7*, 23643–23652.

(17) van der Merwe, J.; Steenekamp, J.; Steyn, D.; Hamman, J. The role of functional excipients in solid oral dosage forms to overcome poor drug dissolution and bioavailability. *Pharmaceutics* **2020**, *12*, 393.

(18) Ciobanu, A.; Landy, D.; Fourmentin, S. Complexation efficiency of cyclodextrins for volatile flavor compounds. *Food Res. Int.* **2013**, *53*, 110–114.

(19) Almagro, L.; Pedreño, M. Á. Use of cyclodextrins to improve the production of plant bioactive compounds. *Phytochem. Rev.* **2020**, *19*, 1061–1080.

(20) Harrison, K. Introduction to polymeric drug delivery systems. *Biomedical Polymers*; Elsevier, 2007, pp 33–56.

(21) Majumder, T.; Biswas, G. R.; Majee, S. B. Hydroxy propyl methyl cellulose: different aspects in drug delivery. *J. Pharm. Pharmacol.* **2016**, *4*, 381–385.

(22) Lee, B.-J.; Ryu, S.-G.; Cui, J.-H. Formulation and release characteristics of hydroxypropyl methylcellulose matrix tablet containing melatonin. *Drug Dev. Ind. Pharm.* **1999**, *25*, 493–501.

(23) Zhong, M.; Xie, F.; Zhang, S.; Sun, Y.; Qi, B.; Li, Y. Preparation and digestive characteristics of a novel soybean lipophilic protein-hydroxypropyl methylcellulose-calcium chloride thermosensitive emulsion gel. *Food Hydrocolloids* **2020**, *106*, 105891.

(24) Inamdar, N. N.; Mourya, V. Applications of Polymers in Delivery of Biologics. *Appl. Polym. Drug Delivery* **2021**, 449–534.

(25) Mendonsa, N.; Almutairy, B.; Kallakunta, V. R.; Sarabu, S.; Thipsay, P.; Bandari, S.; Repka, M. A. Manufacturing strategies to develop amorphous solid dispersions: An overview. *J. Drug Deliv. Sci. Technol.* **2020**, *55*, 101459.

(26) Kothari, K.; Ragoonanan, V.; Suryanarayanan, R. The Role of Drug-Polymer Hydrogen Bonding Interactions on the Molecular Mobility and Physical Stability of Nifedipine Solid Dispersions. *Mol. Pharm.* **2015**, *12*, 162–170.

(27) Auch, C.; Harms, M.; Mäder, K. How changes in molecular weight and PDI of a polymer in amorphous solid dispersions impact dissolution performance. *Int. J. Pharm.* **2019**, *556*, 372–382.

(28) Duarte, A. R. C.; Ferreira, A. S. D.; Barreiros, S.; Cabrita, E.; Reis, R. L.; Paiva, A. A comparison between pure active pharmaceutical ingredients and therapeutic deep eutectic solvents: Solubility and permeability studies. *Eur. J. Pharm. Biopharm.* **2017**, *114*, 296–304.

(29) Zhang, X.; Xing, H.; Zhao, Y.; Ma, Z. Pharmaceutical dispersion techniques for dissolution and bioavailability enhancement of poorly water-soluble drugs. *Pharmaceutics* **2018**, *10*, 74.

(30) Rajput, A.; Kulkarni, M.; Deshmukh, P.; Pingale, P.; Garkal, A.; Gandhi, S.; Butani, S. A key role by polymers in microneedle technology: a new era. *Drug Dev. Ind. Pharm.* **2021**, *47*, 1713–1732.

(31) Fitzpatrick, J.; Barringer, S.; Iqbal, T. Flow property measurement of food powders and sensitivity of Jenike's hopper design methodology to the measured values. *J. Food Eng.* **2004**, *61*, 399–405.

(32) Talegaonkar, S.; Mustafa, G.; Akhter, S.; Iqbal, Z. Design and development of oral oil-in-water nanoemulsion formulation bearing atorvastatin: in vitro assessment. *J. Dispersion Sci. Technol.* **2010**, *31*, 690–701.

(33) Heinz, A.; Gordon, K. C.; McGoverin, C. M.; Rades, T.; Strachan, C. J. Understanding the solid-state forms of fenofibrate—A spectroscopic and computational study. *Eur. J. Pharm. Biopharm.* **2009**, *71*, 100–108.

(34) Li, J.; Chai, H.; Li, Y.; Chai, X.; Zhao, Y.; Zhao, Y.; Tao, T.; Xiang, X. A Three-Pulse Release Tablet for Amoxicillin: Preparation, Pharmacokinetic Study and Physiologically Based Pharmacokinetic Modeling. *PLoS One* **2016**, *11*, No. e0160260.

(35) Novák, M.; Snytytsya, A.; Gedeon, O.; Slepíčka, P.; Procházka, V.; Snytytsya, A.; Blahovec, J.; Hejlová, A.; Čopíková, J. Yeast $\beta(1-3)$, (1-6)-D-glucan films: Preparation and characterization of some structural and physical properties. *Carbohydr. Polym.* **2012**, *87*, 2496–2504.

(36) Songsurang, K.; Pakdeebumrung, J.; Praphairaksit, N.; Muangsin, N. Sustained Release of Amoxicillin from Ethyl Cellulose-Coated Amoxicillin/Chitosan-Cyclodextrin-Based Tablets. *AAPS PharmSciTech* **2011**, *12*, 35–45.

(37) Harsha, S. Pharmaceutical suspension containing both immediate/sustained-release amoxicillin-loaded gelatin nanoparticles: preparation and in vitro characterization. *Drug Des., Dev. Ther.* **2013**, *7*, 1027.

(38) Alam, M. A.; Ali, R.; Al-Jenoobi, F. I.; Al-Mohizea, A. M. Solid dispersions: a strategy for poorly aqueous soluble drugs and technology updates. *Expet Opin. Drug Deliv.* **2012**, *9*, 1419–1440.

(39) Konno, H.; Taylor, L. S. Influence of different polymers on the crystallization tendency of molecularly dispersed amorphous felodipine. *J. Pharm. Sci.* **2006**, *95*, 2692–2705.

(40) Singhvi, G.; Singh, M. In-vitro drug release characterization models. *Int. J. Pharm. Stud. Res.* **2011**, *2*, 77–84.

(41) Jawad, A. H.; Malek, N. N. A.; Abdulhameed, A. S.; Razuan, R. Synthesis of Magnetic Chitosan-Fly Ash/Fe₃O₄ Composite for Adsorption of Reactive Orange 16 Dye: Optimization by Box–Behnken Design. *J. Polym. Environ.* **2020**, *28*, 1068–1082.

(42) Hou, H.; Sun, C. C. Quantifying effects of particulate properties on powder flow properties using a ring shear tester. *J. Pharm. Sci.* **2008**, *97*, 4030–4039.

(43) Agarwal, P.; Goyall, A.; Vaishnav, R. Comparative Quality Assessment of Three Different Marketed Brands of Indian Polyherbal Formulation—Triphala Churna. *Biomed. J. Sci. Technol. Res.* **2018**, *2582*, 7421.

(44) Amin, S.; Sher, M.; Ali, A.; Rehman, M. F.; Hayat, A.; Ikram, M.; Abbas, A.; Amin, H. M. A. Sulfonamide-functionalized silver nanoparticles as an analytical nanoprobe for selective Ni(II) sensing with synergistic antimicrobial activity. *Environ. Nanotechnol. Monit. Manag.* **2022**, *18*, 100735.

(45) Irfan, M. I.; Amjad, F.; Abbas, A.; Rehman, M. F.; Kanwal, F.; Saeed, M.; Ullah, S.; Lu, C. Novel Carboxylic Acid-Capped Silver Nanoparticles as Antimicrobial and Colorimetric Sensing Agents. *Molecules* **2022**, *27*, 3363.

(46) Bilal, S.; Sami, A. J.; Hayat, A.; Fayyaz ur Rehman, M. F. Assessment of pesticide induced inhibition of Apis mellifera (honeybee) acetylcholinesterase by means of N-doped carbon dots/BSA nanocomposite modified electrochemical biosensor. *Bioelectrochemistry* **2022**, *144*, 107999.

(47) Malik, A.; Khan, A.; Mahmood, Q.; Nawaz Marth, M. M. A.; Riaz, M.; Tabassum, T.; Rasool, G.; Rehman, M. F. u.; Batool, A. I.; Kanwal, F.; et al. In Vivo and In Silico Assessment of the

Cardioprotective Effect of *Thymus linearis* Extract against Ischemic Myocardial Injury. *ACS Omega* **2022**, *7*, 43635–43646.

(48) Sher, M.; Hameed, A.; Noreen, S.; Fayyaz-ur-Rehman, M.; Hussain, M. A.; Bukhari, S. N. A. Extraction, purification and characterization of the crystallin protein of cataractous eye lens nucleus. *Analyst* **2015**, *140*, 6392–6397.